DOI: 10.1002/asia.200600113

# Tuning the Formation of Cadmium(II) Urocanate Frameworks by Control of Reaction Conditions: Crystal Structure, Properties, and Theoretical Investigation

**Ru-Qiang Zou,[a, b] Rui-Qin Zhong,[a, b] Ling Jiang,[a, b] Yusuke Yamada,[a] Nobuhiro Kuriyama,[a] and Qiang Xu*[a, b]**

**Abstract:** The reaction of cadmium(II) perchlorate with urocanic acid under different conditions created three novel coordination compounds: $[Cd_2(L^2)_2(L^3)_2(H_2O)_8]$ (**1**), $\{[Cd(L)(L^2)](H_2O)_{1/2}\}_n$ (**2**), and $\{[Cd(L^3)_2](H_2O)_{3/2}(EtOH)\}_n$ (**3**), in which L, $L^2$, and $L^3$ are three urocanate tautomers. Complex **1** consists of two separate mononuclear units with different urocanate tautomers, which self-assemble into a 3D hydrogen-bonding network constructed by alternating 2D layers, whereas complexes **2** and **3** self-assemble into 3D alpha-polonium and four-fold interpenetrated diamondoid networks, respectively. The tautomerism of the urocanate ligands and the enormous structural diversity of their complexes are present in this system, which illustrates that the reaction temperature, pressure, and the metal ions themselves act cooperatively to tune the tautomerism of the ligands and the frameworks of their metal coordination compounds. The fluorescence-emission and nitrogen-adsorption properties of these complexes are also investigated.

**Keywords:** alpha-polonium networks · cadmium · diamondoid networks · tautomerism · urocanate ligands

## Introduction

The enormous structural diversity exhibited by metal–organic frameworks represents an opportunity and a challenge for the crystal engineering of materials with new structural motifs.[1] It is well-known that their topologies can often be controlled and modulated by the selection of the coordination geometry of the metal ions,[2] the chemical nature of organic ligands,[3] the polarity of reaction solvent,[4] reaction temperature,[5] the use of template molecules,[6] and so on. On the other hand, the structural diversity of these frameworks, especially for a given set of components, is of particular importance because the superstructure plays an essential role in determining the properties of crystalline solids.[7]

Herein, we successfully synthesized and characterized a discrete mononuclear entity and two novel 3D metal–organic frameworks with urocanate ligands, $[Cd_2(L^2)_2(L^3)_2(H_2O)_8]$ (**1**), $\{[Cd(L)(L^2)](H_2O)_{1/2}\}_n$ (**2**), and $\{[Cd(L^3)_2](H_2O)_{3/2}(EtOH)\}_n$ (**3**) (HL–$HL^3$ are shown in Scheme 1), by controlling the reaction conditions. Notably, the rotations of the carboxy group and the imidazolyl ring (HL and $HL^1$, $HL^2$ and $HL^3$) allow different coordination geometries of the li-

[a] R.-Q. Zou, R.-Q. Zhong, L. Jiang, Dr. Y. Yamada, Dr. N. Kuriyama, Prof. Dr. Q. Xu
National Institute of Advanced Industrial Science and Technology (AIST)
Ikeda, Osaka 563-8577 (Japan)

[b] R.-Q. Zou, R.-Q. Zhong, L. Jiang, Prof. Dr. Q. Xu
Graduate School of Science and Technology
Kobe University
Nada Ku, Kobe, Hyogo 657-8501 (Japan)
Fax: (+81) 72-751-9629
E-mail: q.xu@aist.go.jp

Supporting information for this article is available on the WWW under http://www.chemasianj.org or from the author.

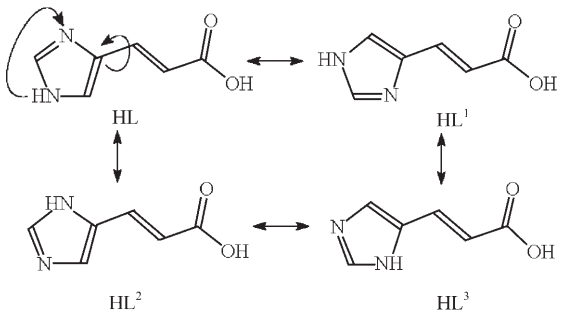


Scheme 1. The four urocanic acid tautomers HL–$HL^3$.

gands. More importantly, H transfer between the two N atoms of the imidazolyl group (HL and $HL^2$, $HL^1$ and $HL^3$) caters to the coordination needs of the metal ions (Scheme 1). As a result, although we used HL as reagent with $\geq 99\,\%$ assay and employed the same solvent, its deprotonated tautomers ($L^2$ and $L^3$) were also present in the coordination compounds through rotation of and H transfer in the imidazolyl ring (Scheme 2). This suggests that the reaction temperature, pressure, and the metal ions act as cooperatively to control the tautomers of the ligand, resulting in the structural diversity of their metal coordination polymers.

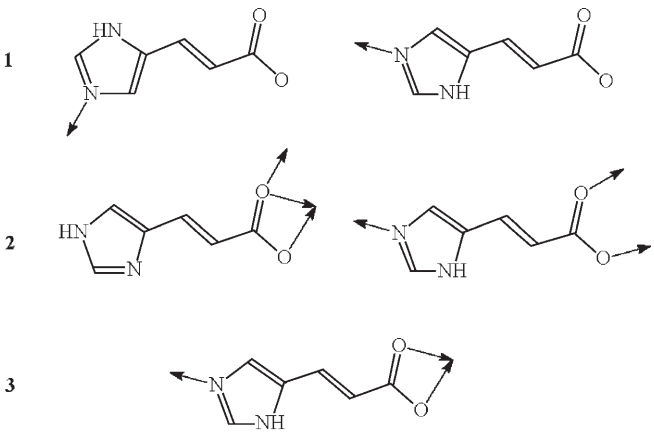


Scheme 2. The ligand coordination modes in complexes **1**–**3**.

## Results and Discussion

### Description of Crystal Structures

The crystallographic data and details of the structure refinement for complexes **1**–**3** are summarized in Table 1.

Complex **1** crystallizes in the monoclinic space group $P2_1/n$. The crystal structure contains two separate mononuclear units, $[Cd(L^2)_2(H_2O)_4]$ and $[Cd(L^3)_2(H_2O)_4]$, with tautomeric urocanate ligands ($L^2$ and $L^3$) (Figure 1 a). The two types of $Cd^{II}$ center both adopt octahedral geometries

Table 1. Crystallographic data and structure refinement for **1**–**3**.

| | **1** | **2** | **3** |
|---|---|---|---|
| Chemical formula | $C_{12}H_{18}CdN_4O_8$ | $C_{12}H_{11}CdN_4O_{4.50}$ | $C_{28}H_{38}Cd_2N_8O_{13}$ |
| $M_r$ | 458.70 | 395.65 | 919.46 |
| Space group | $P2_1/n$ | $C2/c$ | $I4_1/a$ |
| $a$ [Å] | 12.0260(10) | 12.4153(11) | 18.6378(19) |
| $b$ [Å] | 7.2880(6) | 13.7177(12) | 18.6378(19) |
| $c$ [Å] | 17.8803(14) | 15.0099(16) | 22.570(3) |
| α [°] | 90 | 90 | 90 |
| β [°] | 93.0860(10) | 94.3440(10) | 90 |
| γ [°] | 90 | 90 | 90 |
| $V$ [Å$^3$] | 1564.9(2) | 2549.0(4) | 7840.2(15) |
| $Z$ | 4 | 8 | 8 |
| GOF | 1.080 | 1.043 | 1.212 |
| $D$ [g cm$^{-3}$] | 1.947 | 2.062 | 1.558 |
| μ [mm$^{-1}$] | 1.449 | 1.742 | 1.152 |
| $T$ [K] | 183(2) | 293(2) | 273(2) |
| $R^{[a]}/wR^{[b]}$ | 0.0227/0.0642 | 0.0212/0.0527 | 0.0754/0.1339 |

[a] $R=\Sigma(||F_0|-|F_C||)/\Sigma|F_0|$; [b] $wR=[\Sigma w(|F_0|^2-|F_C|^2)^2/\Sigma w(F_0^2)]^{1/2}$.

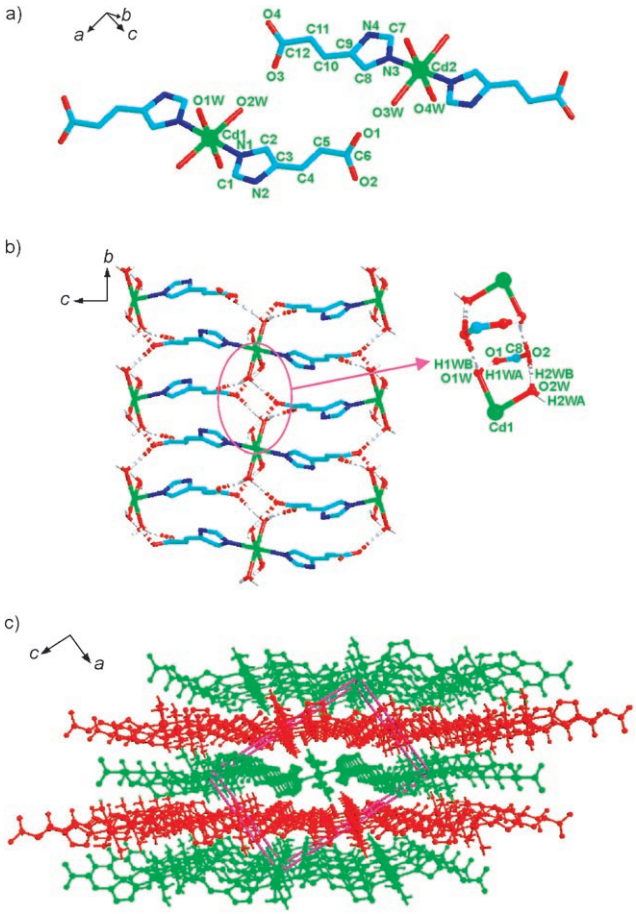


Figure 1. a) The two separate mononuclear units with H atoms omitted, b) the quasi-2D network consisting of intermolecular hydrogen-bonding interactions, and c) the packing pattern of the 2D hydrogen-bonding networks of **1**. ● = Cd, ● = C, ● = N, ● = O, ○ = H.

through the coordination of two imidazolyl nitrogen atoms from two symmetric urocanate ligands and four water molecules. The carboxy group of each urocanate ligand does not coordinate to the $Cd^{II}$ center. The Cd–N and Cd–O bonds lengths are within the normal ranges (Table 2).[10]

The two types of mononuclear unit $[Cd(L^2)_2(H_2O)_4]$ and $[Cd(L^3)_2(H_2O)_4]$ self-assemble into similar 2D layers through hydrogen bonding with the opposite urocanate tautomer. The related hydrogen-bonding geometry is given in Table 3. All the hydrogen-bond distances fall within the normal range. Figure 1 b shows the 2D hydrogen-bonding layer constructed by the adjacent $[Cd(L^2)_2(H_2O)_4]$ units. The intermolecular O–H···O hydrogen-bonding interactions O1W–H1WB···O2#2 (#2 = $x-1$, $-y+1.5$, $z+0.5$), O1W–H1WA···O1#7 (#7 = $-x+1$, $y+0.5$, $-z+0.5$), and O2W–H2WB···O2#6 (#6 = $x-1$, $-y+0.5$, $z+0.5$) from the coordinated $H_2O$ and $COO^-$ groups of the $[Cd(L^2)_2(H_2O)_4]$ unit lead to the formation of the 2D layer, which is parallel to the [100] and [010] directions. There is a similar 2D hydrogen-bonding layer constructed by $[Cd(L^3)_2(H_2O)_4]$ units. Furthermore, these two similar types of layers are alternately arranged to form a 3D network (Figure 1 c) with intermolecular hydrogen-bonding interactions (Table 3).

  

Table 2. Selected bond lengths (Å) and angles (°) for **1**.[a]

| | | | |
|---|---|---|---|
| Cd1–N1 | 2.2850(13) | Cd1–O2W | 2.2955(12) |
| Cd1–O1W | 2.3770(12) | Cd2–N3 | 2.2264(13) |
| Cd2–O3W | 2.3452(12) | Cd2–N3 | 2.3643(12) |
| | | | |
| N1–Cd1–N1#1 | 180.00(7) | Cd1–O2W | 91.34(5) |
| N1–Cd1–O2W | 88.66(5) | O2W#1–Cd1–O2W | 180.0 |
| N1–Cd1–O1W | 95.42(4) | N1#1–Cd1–O1W | 84.58(4) |
| O2W#1–Cd1–O1W | 84.54(4) | O2W–Cd1–O1W | 95.46(4) |
| O1W–Cd1–O1W#1 | 180.0 | N3#2–Cd2–N3 | 180.0 |
| N3#2–Cd2–O3W | 93.76(5) | N3–Cd2–O3W | 86.24(5) |
| O3W–Cd2–O3W#2 | 180.00(6) | N3#2–Cd2–O4W#2 | 94.68(4) |
| N3–Cd2–O4W#2 | 85.32(5) | O3W–Cd2–O4W#2 | 89.94(4) |
| O3W–Cd2–O4W | 90.07(4) | O4W#2–Cd2–O4W | 180.0 |

[a] Symmetry codes for **1**: #1 = $-x+2,-y+2,-z$; #2 = $-x,-y,-z+1$.

Table 3. Hydrogen-bonding geometries for **1**.

| D–H···A[a] | D–H [Å] | H···A [Å] | D···A [Å] | D–H···A [°] |
|---|---|---|---|---|
| O4W–H4WB···O4#1 | 0.82 | 1.98 | 2.774(2) | 166 |
| O1W–H1WB···O2#2 | 0.82 | 2.14 | 2.933(2) | 165 |
| N2–H2A···O3 | 0.83 | 1.94 | 2.771(2) | 179 |
| O3W–H3WA···O2#3 | 0.83 | 1.90 | 2.722(1) | 176 |
| O2W–H2WA···O4#4 | 0.82 | 1.88 | 2.698(2) | 175 |
| N4–H4A···O1#5 | 0.89 | 1.92 | 2.805(9) | 174 |
| O2W–H2WB···O2#6 | 0.81 | 2.02 | 2.827(0) | 172 |
| O3W–H3WB···O4# 6 | 0.84 | 2.02 | 2.833(9) | 162 |
| O1W–H1WA···O1#7 | 0.82 | 1.89 | 2.693(5) | 165 |
| O4W–H4WA···O3#3 | 0.82 | 1.87 | 2.687(4) | 171 |
| C1–H1···O2W | 0.95 | 2.55 | 3.143(5) | 121 |
| C4–H4···O4W#4 | 0.95 | 2.58 | 3.515(3) | 168 |
| C7–H7···O3W | 0.95 | 2.52 | 3.097(6) | 119 |
| C11–H11···O1W#3 | 0.95 | 2.58 | 3.427(3) | 148 |

[a] Symmetry codes: #1 = $x-1$, $-y-0.5$, $z+0.5$; #2 = $x-1$, $-y+1.5$, $z+0.5$; #3 = $-x$, $y-0.5$, $-z+0.5$; #4 = $-x$, $y+0.5$, $-z+0.5$; #5 = $x-1$, $y$, $z$; #6 = $x-1$, $-y+0.5$, $z+0.5$; #7 = $-x+1$, $y+0.5$, $-z+0.5$.

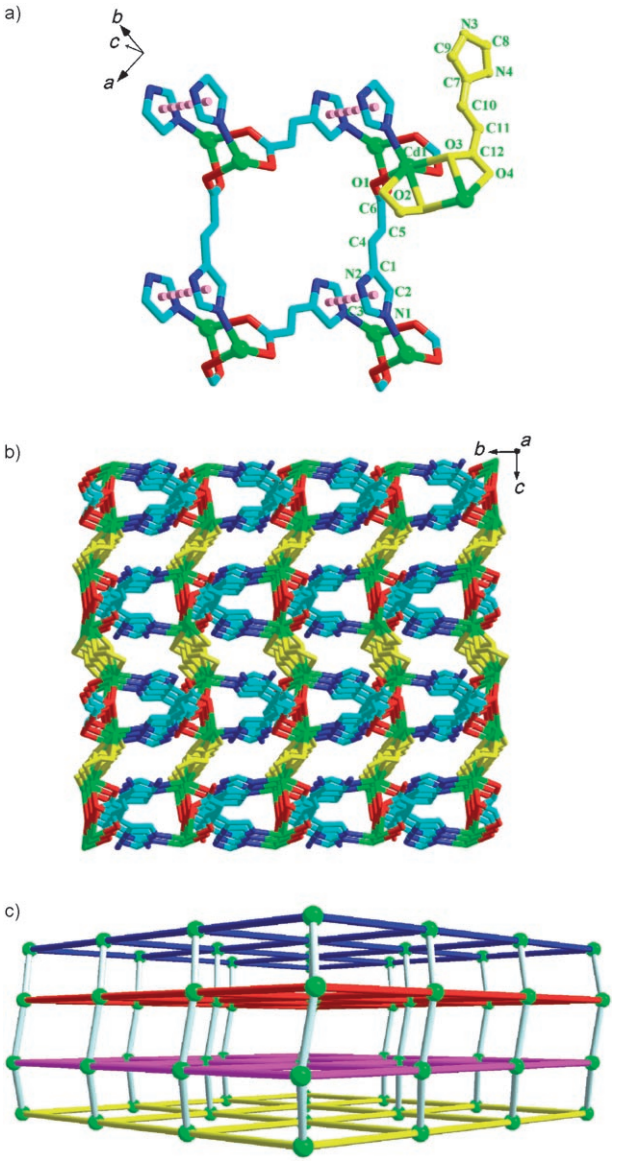


Figure 2. Sections of the polymeric structures of **2** showing a) the unique octanuclear building blocks bridged by the carboxy groups of L (yellow), b) the 3D framework consisting of the adjacent 2D layers bridged by the carboxy groups of L, and c) a schematic illustration of the alpha-polonium network. ● = Cd, ● = C, ● = N, ● = O, ● shows the centroid-to-centroid separation of two imidazolyl rings.

Complex **2** crystallizes in the monoclinic space group *C2/c*. The asymmetric unit of **2** contains one $Cd^{II}$ center, the mixed urocanate ligands (L and $L^2$), and half a water molecule. The $Cd^{II}$ center adopts a distorted octahedral geometry by coordinating to an imidazolyl nitrogen atom and four carboxy groups of L and $L^2$ in a chelating, $\mu_2$, or monodentate fashion (Figure 2a). The carboxy group of each $L^2$ ligand adopts an O–C–O bridging coordination mode to link two adjacent $Cd^{II}$ ions and form an eight-membered dimetallocycle with a Cd···Cd separation of 4.102 Å, whereas that from each L ligand adopts $\mu_2$ and monodentate coordination modes to link two adjacent $Cd^{II}$ ions and form a four-membered dimetallocycle with a Cd···Cd separation of 3.856 Å. The two types of dimetallocycle share the $Cd^{II}$ centers and expand in an infinite chain down the *c* axis. The imidazolyl N atoms of $L^2$ are coordinated to the $Cd^{II}$ centers, whereas those of L are not. Notably, the reagent HL became $L^2$ to coordinate to $Cd^{II}$ centers through H transfer. All the Cd–O and Cd–N bond lengths fall within the normal ranges (Table 4).[10]

A more-careful examination shows that the structure of **2** contains a 2D layer constructed by unique octanuclear cadmium building blocks (Figure 2a). In each building block, the two cadmium atoms at each corner are bridged by two carboxy groups of the uraconate ligands to form an eight-membered ring with a Cd···Cd separation of 4.102 Å. The adjacent imidazolyl rings (corresponding symmetry code: $-x+1$, $y$, $0.5-z$) are arranged face-to-face with a centroid-to-centroid separation of 3.382 Å, which indicates the presence of strong π–π stacking interactions. Interestingly, the carboxy groups of L link these adjacent 2D layers to form a

  

Table 4. Selected bond lengths (Å) and angles (°) for **2**.[a]

| | | | |
|---|---|---|---|
| Cd1–N1 | 2.2248(17) | Cd1–O2#1 | 2.2610(14) |
| Cd1–O4#2 | 2.3647(16) | Cd1–O1#3 | 2.3684(16) |
| Cd1–O3#2 | 2.3904(15) | Cd1–O3 | 2.4489(16) |
| Cd1–C12#2 | 2.725(2) | | |
| | | | |
| N1–Cd1–O2#1 | 126.25(6) | N1–Cd1–O4#2 | 92.96(6) |
| O2#1–Cd1–O4#2 | 140.69(6) | N1–Cd1–O1#3 | 97.97(6) |
| O2#1–Cd1–O1#3 | 87.89(5) | O4#2–Cd1–O1#3 | 83.40(6) |
| N1–Cd1–O3#2 | 142.12(6) | O2#1–Cd1–O3#2 | 88.30(5) |
| O4#2–Cd1–O3#2 | 55.51(6) | O1#3–Cd1–O3#2 | 98.35(5) |
| N1–Cd1–O3 | 94.38(6) | O2#1–Cd1–O3 | 80.97(6) |
| O4#2-Cd1-O3 | 100.71(6) | O1#3–Cd1–O3 | 166.77(6) |
| O3#2–Cd1–O3 | 74.33(6) | | |

[a] Symmetry codes for **2**: #1 = $-x+0.5$, $y-0.5$, $-z+0.5$; #2 = $-x$, $-y+1$, $-z+1$; #3 = $x-0.5$, $y-0.5$, $z$.

noninterpenetrated 3D alpha-polonium network (Figure 2b).[11] The two nearest cadmium atoms between two adjacent 2D layers are bridged by two carboxy oxygen atoms from L through $\mu_2$ coordination to form a four-membered dimetallocycle with a Cd···Cd separation of 3.856 Å. Figure 2c shows the continuous and slightly distorted rectilinear alpha-polonium network with each cadmium atom pair in the eight-membered ring of the octanuclear unit as a node. Thus, it is reasonable that the 3D alpha-polonium network of **2** consists of 2D layers with unique octanuclear cadmium building blocks that are bridged by the carboxy groups of L. The water molecules are included in the spaces between two adjacent layers with strong intermolecular hydrogen-bonding interactions (Table 5).

Table 5. Hydrogen-bonding geometries for **2**.[a]

| D–H···A | D–H [Å] | H···A [Å] | D···A [Å] | D–H···A [Å] |
|---|---|---|---|---|
| N2–H2A···N4#1 | 0.86 | 2.04 | 2.895(8) | 171 |
| N3–H3 A···O1W#2 | 0.86 | 2.53 | 2.901(1) | 107 |
| N3–H3A···O2#3 | 0.86 | 1.95 | 2.780(0) | 160 |
| C2–H2···O1#4 | 0.93 | 2.46 | 3.082(0) | 125 |
| C3–H3···O1W#5 | 0.93 | 2.27 | 3.134(9) | 154 |
| C5–H5···O1W#6 | 0.93 | 2.55 | 3.213(0) | 129 |
| C8–H8···O1W#2 | 0.93 | 2.60 | 2.933(0) | 102 |
| C9–H9···O3#7 | 0.93 | 2.59 | 3.295(5) | 133 |
| C10–H10···O3 | 0.93 | 2.43 | 2.793(6) | 103 |

[a] Symmetry codes: #1 = $x-0.5$, $y+0.5$, $z$; #2 = $-x+1$, $-y+1$, $-z+1$; #3 = $-x+1$, $y$, $-z+0.5$; #4 = $-x+0.5$, $y-0.5$, $-z+0.5$; #5 = $-x$, $y+1$, $-z+1$; #6 = $x$, $-y+1$, $z-0.5$; #7 = $-x+0.5$, $-y+1.5$, $-z+1$.

Under solvothermal conditions at 140 °C, the reaction of HL with $Cd(ClO_4)_2 \cdot 6H_2O$ affords the four-fold interpenetrated diamondoid network of **3**; a similar structure was recently reported with different guest molecules.[12] The crystal data of **3** were collected with low-temperature refinement and well-refined guest molecules ($H_2O$ and EtOH).

As opposed to **1** and **2**, complex **3** crystallizes in the high-symmetry tetragonal space group $I4_1/a$. The asymmetric unit of **3** contains one $Cd^{II}$ center, two $L^3$ ligands, and one and a half water and one ethanol molecules. The $Cd^{II}$ center adopts a highly distorted octahedral geometry through coordination of two imidazolyl nitrogen atoms and two chelating carboxy groups from four separate $L^3$ ligands (Figure 3a). If the chelating carboxy groups are treated as connecting points, the $Cd^{II}$ centers in **3** have a pseudotetrahedral geometry. Each $Cd^{II}$ center in **3** is thus connected to four other $Cd^{II}$ centers to produce a diamondoid network (Figure 3a). With Cd···Cd separations of 10.823 and 10.967 Å, a large void is generated within a single diamondoid cage. Each $L^3$ ligand links two adjacent $Cd^{II}$ ions and expands in three dimensions to form the nanosized (≈19 Å) channel structure

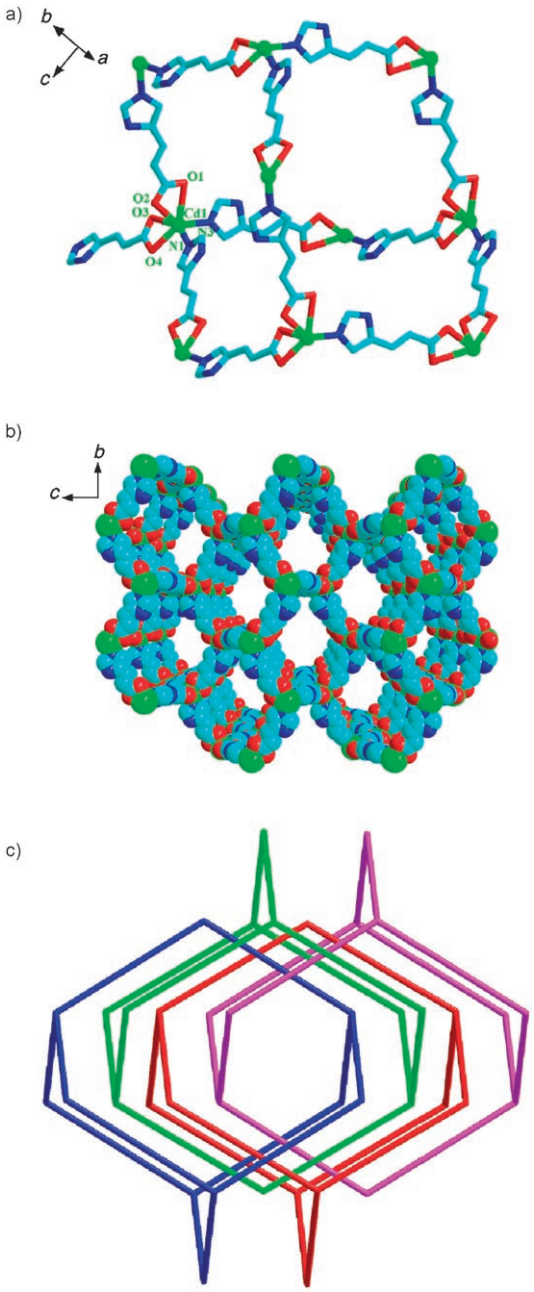


Figure 3. a) The diamondoid network unit, b) the 3D framework with nanosized open channels along the *a* axis, and c) diagram illustrating the four-fold interpenetration along the *a* axis of **3**. ● = Cd, ● = C, ● = N, ● = O.

(Figure 3b). Notably, the cavities are decreased in size by three other identical interpenetrated diamondoid networks, such that four independent diamondoid networks mutually interpenetrate (Figure 3c). All the Cd–O and Cd–N bond lengths fall within the normal ranges (Table 6).[10] Complex

Table 6. Selected bond lengths (Å) and angles (°) for **3**.[a]

| | | | |
|---|---|---|---|
| Cd1–N3 | 2.192(6) | Cd1–O2#1 | 2.241(5) |
| Cd1–N1#2 | 2.251(7) | Cd1–O4 | 2.285(5) |
| Cd1–O3 | 2.459(5) | Cd1–O1#1 | 2.608(5) |
| Cd1–C6 | 2.735(7) | | |
| | | | |
| N3–Cd1–O2#1 | 139.4(2) | N3–Cd1–N1#2 | 103.3(2) |
| O2#1–Cd1–N1#2 | 93.9(2) | N3–Cd1–O4 | 116.9(2) |
| O2#1–Cd1–O4 | 97.0(2) | N1#2–Cd1–O4 | 96.0(2) |
| N3–Cd1–O3 | 96.8(2) | O2#1–Cd1–O3 | 84.20(19) |
| N1#2–Cd1–O3 | 150.55(19) | O4–Cd1–O3 | 55.34(17) |
| N3–Cd1–O1#1 | 86.9(2) | O2#1–Cd1–O1#1 | 52.95(18) |
| N1#2–Cd1–O1#1 | 104.8(2) | O4–Cd1–O1#1 | 143.78(18) |
| O3–Cd1–O1#1 | 97.40(18) | | |

[a] Symmetry codes for **3**: #1 = $x$, $y-0.5$, $-z$; #2 = $x-0.5$, $y$, $-z+0.5$; #3 = $x+0.5$, $y$, $-z+0.5$.

**3** belongs to class IIa of interpenetration,[1g,13,14] in which the networks are related by a single symmetry element. Only a few examples of this type of four-fold interpenetration have been reported.[12,15,16] Despite the nature of the interpenetration, **3** still forms 1D open channels ($10.8\times11.0$ Å$^2$) in which guest molecules (EtOH and $H_2O$) are trapped (Table 7).

Table 7. Hydrogen-bonding geometries for **3**.[a]

| D–H···A | D–H [Å] | H···A [Å] | D···A [Å] | D–H···A [Å] |
|---|---|---|---|---|
| O1W–H1WB···O4 | 0.82 | 2.13 | 2.755(3) | 133 |
| N2–H2D···O3#1 | 0.86 | 1.98 | 2.799(8) | 158 |
| O2W–H2WA···O1W | 1.10 | 2.00 | 3.001(0) | 149 |
| N4–H4D···O2#2 | 0.86 | 1.86 | 2.684(2) | 159 |
| C3–H3···O1#3 | 0.93 | 2.44 | 3.338(2) | 161 |
| C4–H4···O3 | 0.93 | 2.52 | 2.840(8) | 101 |
| C9–H9···O1#4 | 0.93 | 2.45 | 3.097(8) | 127 |
| C11–H11···N4 | 0.93 | 2.59 | 2.917(7) | 101 |
| C13–H13B···O1W#5 | 0.96 | 1.92 | 2.805(9) | 152 |
| C13–H13C···O1W | 0.96 | 1.99 | 2.796(8) | 140 |

[a] Symmetry codes: #1 = $-y+0.75$, $x+0.25$, $z+0.25$; #2 = $y+0.25$, $-x+1.25$, $z+1.25$; #3 = $-x+0.5$, $-y+1.5$, $-z+0.5$; #4 = $x$, $y-0.5$, $-z$; #5 = $-x+0.75$, $y-0.25$, $z-0.5$.

### Thermogravimetric Analysis

Thermogravimetric analysis (TGA) was carried out to investigate the thermal stabilities of **2** and **3** (see Supporting Information). The TGA curve of **2** indicates the slow release of guest molecules ($H_2O$) up to about 200 °C to give the solvent-free form; this slow release is probably due to the strong hydrogen-bonding interactions of the trapped water molecules with the urocanate ligands. From 300 °C, the ligands start to be released. The TGA curve of **3** indicates the release of guest molecules ($H_2O$ and EtOH) from 80 to 160 °C to give its solvent-free form. From 290 °C, the ligands start to be released. Furthermore, the powder XRD patterns of **1**–**3** also indicate that only one clean phase is formed at each reaction condition.

### Fluorescence Emission

The fluorescence emission properties of **1**–**3** and urocanic acid were further investigated. Urocanic acid displays a weak fluorescence maximum at 380 nm in the solid state at room temperature, whereas **2** exhibits an intense bathochromic shift with the emission maximum at 483 nm ($\lambda_{ex}=$ 380 nm) (Figure 4). The bathochromic shift is undoubtedly

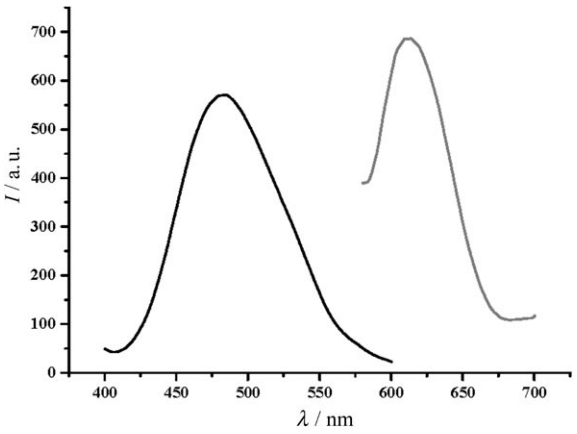


Figure 4. Fluorescence emission spectra of **2** and **3** in the solid state with $\lambda_{ex}=380$ nm for **2** and $\lambda_{ex}=460$ nm for **3**. ——= **2**, ——= **3**.

due to the deprotonation of the ligand when forming the 3D alpha-polonium network. The π–π stacking interactions of the imidazolyl groups may have also contributed to the bathochromic shift in **2**. Complex **3** displays an intense emission maximum at 612 nm ($\lambda_{ex}=460$ nm) (Figure 4), which may be attributed to metal-to-ligand charge transfer (MLCT). Undoubtedly, the rigidity of the frameworks of **3** also contributes to the enhancement of the fluorescence emission.[17] Complex **1** exhibits a slightly weaker fluorescence emission than that of free urocanic acid, which may be attributed to the many coordinated water molecules in **1** quenching the fluorescence emission of the ligands. The strong blue emissions of **2** and **3** in the solid state implies that these complexes may be potentially applicable as materials for blue-light-emitting diode devices.[18]

### Nitrogen Adsorption

Despite the nature of the four-fold interpenetration, **3** still forms 1D open channels in which guest molecules (EtOH and $H_2O$) are trapped. The total potential void volumes of the open channels of **3** are estimated to be about 35.3% (2769.7 Å$^3$) of the volume of the unit cell (7840.2 Å$^3$), as calculated with PLATON.[19] The powder XRD patterns and crystal structure of the dehydrated form of **3** also confirmed that the solids, after removal of the solvent molecules, retain

  

the initial framework of **3**.[12] Therefore, it is possible to study the molecular adsorption features of **3**.

The nitrogen adsorption behavior of **3** was examined at 77 K. Nitrogen adsorption isotherms were recorded with automatic volumetric adsorption equipment (ASAP2010, Micrometritics). A sample of **3** (330 mg) was placed in a quartz tube and dried under high vacuum at 160 °C for 10 h to remove the solvent molecules prior to measurements. Approximately 1.08 mmol of $N_2$ per gram of solvent-free sample was adsorbed at 1 atm (Figure 5).

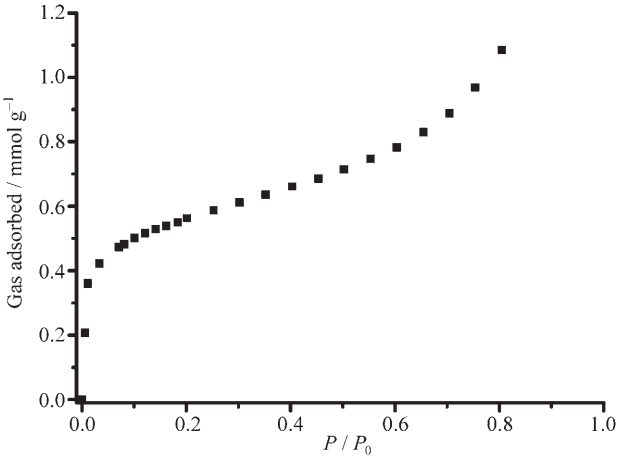


Figure 5. $N_2$ adsorption curve of **3** at 77 K.

## Theoretical Investigations

To provide insight into the energy difference and charge distribution of **1**–**3**, we performed quantum chemical calculations with the Gaussian 03 program.[20] The Becke three parameter hybrid functional with the Lee–Yang–Parr correlation corrections (B3LYP) was used.[21] The 6-311+G(d) basis set was used for C, N, O, and H atoms, and the Los Alamos ECP plus DZ (LANL2DZ) for Cd atoms.[22] For the tautomers of HL–HL$^3$, the geometries were fully optimized, and vibrational frequencies were calculated with analytical second derivatives. For **2** and **3**, Mulliken population analysis was carried out on the geometries of the monomolecular units cut out from the crystal data.

Figure 6 shows the optimized structures, selected Mulliken charge distributions, and relative energies of the HL tautomers. The energy differences of the imidazolyl H transfer between HL and HL$^2$ ($\Delta E = 0.27$ kcal mol$^{-1}$) and between HL$^1$ and HL$^3$ ($\Delta E = -0.34$ kcal mol$^{-1}$) are lower than those of the rotation of the imdazolyl group between HL and HL$^1$ ($\Delta E = 1.73$ kcal mol$^{-1}$) and between HL$^2$ and HL$^3$ ($\Delta E = 1.12$ kcal mol$^{-1}$), all of which are small. On the other hand, $^1$H NMR spectroscopic measurements showed that upon heating HL to 90 and 140 °C in water without Cd$^{II}$ ions, it does not turn tautomerize, which suggests high activation barriers for H transfer and imidazole ring flip. As shown in Figure 7, the lowest unoccupied and highest occupied molecular orbitals (LUMO and HOMO, respectively) of singlet HL further imply that the C–C bonds between the imidazolyl and alkenyl groups are tightened by the conjugated π system, which makes the imidazole ring difficult to flip. The observation of the tautomers herein suggests that the Cd$^{II}$ ions play an important role in determining the structures of urocanate ligands. In **1**, HL turns into HL$^2$ and HL$^3$ to coor-

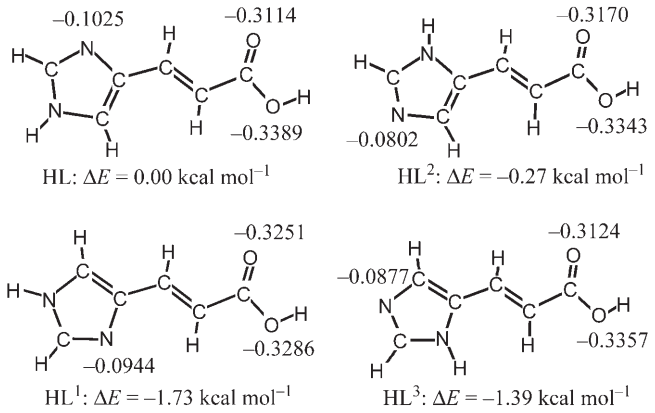


Figure 6. Optimized structures, selected Mulliken charge distributions, and relative energies of the urocanic acid tautomers at the B3LYP/6-311+G(d) level of theory.

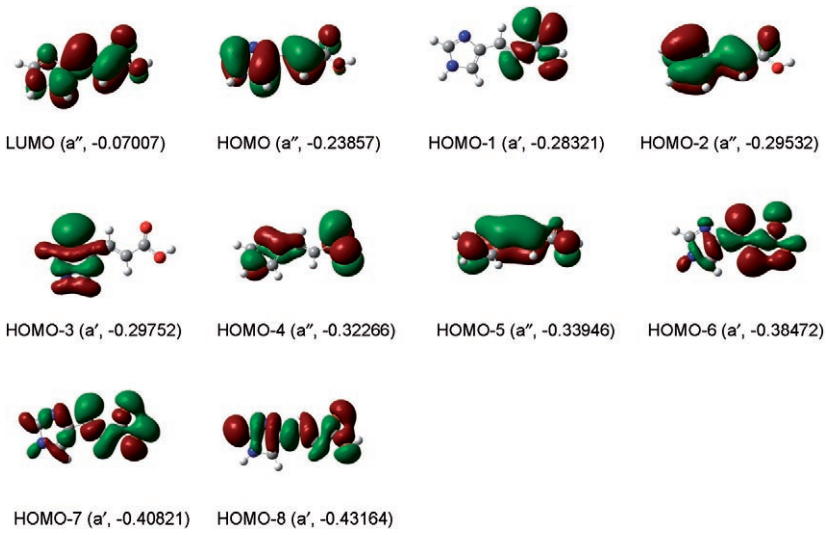


Figure 7. Molecular orbital pictures of singlet HL, showing the LUMO and HOMOs down to the eighth valence molecular orbital from the HOMO. The unit of orbital energy is the hartree (in parentheses).

dinate to $Cd^{II}$ ions at room temperature as it is energetically favorable. Calculations on the asymmetric units of **2** and **3** at the B3LYP/6–311+G(d)-LANL2DZ level predict that **3** lies 30.59 kcal mol$^{-1}$ lower in energy than **2**, which suggests that **3** has a more stable structure than **2**. Furthermore, **3** was only obtained under higher-temperature solvothermal conditions herein, thus implying that the tautomerism of the ligands results from a cooperative effect of the temperature, pressure, and the metal ions in the self-assembly (Scheme 3).

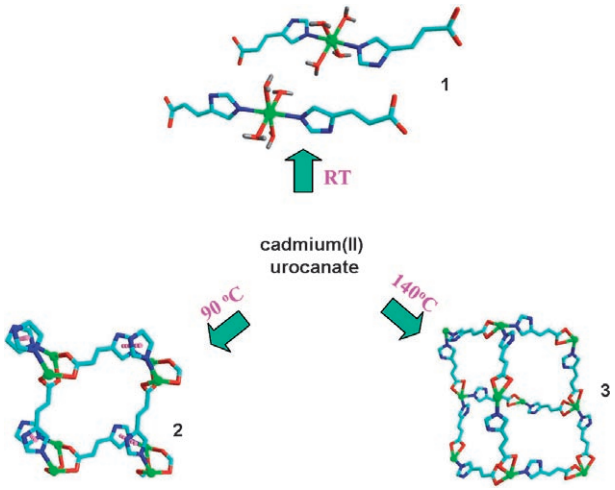


Scheme 3. Schematic illustration of the three cadmium urocanate compounds.

## Conclusions

Three $Cd^{II}$ urocanate coordination compounds have been synthesized separately through control of the reaction conditions. The tautomers of the urocanate ligand were present in this system, which illustrates that the temperature, pressure, and the metal ions act cooperatively to control the tautomerism of the ligands. This effect results in the enormous structural diversity of such metal coordination compounds.

## Experimental Section

*Materials and General Methods*

All the solvents and reagents for synthesis were commercially available and used as received. FTIR spectra (KBr pellets) were recorded on a JASCO FT/IR-230 spectrometer. Powder XRD data was collected with $Cu_{K\alpha}$ ($\lambda = 1.5406$ Å) radiation on a Rigaku X-ray diffractometer. TGA was carried out at a ramp rate of 5 °C min$^{-1}$ in a helium atmosphere with a Shimadzu DTG-50 instrument. Emission spectra were recorded on a Perkin–Elmer LS50B luminescence spectrophotometer. Nitrogen adsorption measurements were performed with automatic volumetric adsorption equipment (ASAP2010, Micrometritics).

*Syntheses*

**1**: A mixture of $Cd(ClO_4)_2 \cdot 6H_2O$ (0.84 g, 2 mmol), urocanic acid (0.28 g, 2 mmol), and a solution of water/ethanol/pyridine (1:5:1, 10 mL) was stirred for 3 h and filtered. Colorless crystals of **1** (0.29 g, ≈63 %) were obtained after the filtrate was left to stand for ten days at room temperature. IR (KBr): $\tilde{\nu} = 3357$ (m), 2854 (w), 1653 (s), 1529 (vs), 1384 (vs), 1277 (m), 1166 (s), 1124 (vs), 1001 (s), 846 (m), 678 (m), 647 cm$^{-1}$ (m).

**2**: A mixture of $Cd(ClO_4)_2 \cdot 6H_2O$ (0.84 g, 2 mmol), urocanic acid (0.28 g, 2 mmol), and water/ethanol/pyridine (1:5:1, 10 mL) was sealed in a teflon-capped scintillation vial. Yellow prismatic crystals of **2** (0.14 g, ≈36 %) were obtained after four days of heating at 90 °C. IR (KBr): $\tilde{\nu} =$ 3132 (m), 1845 (vs), 1773 (vs), 1696 (s), 1517 (s), 1457 (m), 1276 (m), 840 (m), 701 (w), 624 cm$^{-1}$ (w).

**3**: The synthesis of **3** is similar to that of **2** except that a reaction temperature of 140 °C was used. Colorless block crystals of **3** (0.32 g, ≈70 %) were obtained after four days. IR (KBr): $\tilde{\nu} = 3384$ (m), 1918 (m), 1792 (vs), 1684 (s), 1623 (m), 1534 (s), 1329 (m), 1121 (m), 970 (m), 970 (w), 825 cm$^{-1}$ (w).

Caution: Perchlorate complexes of metal ions in the presence of organic ligands are potentially explosive. These materials should be handled with extreme care in small amounts.

*XRD Data Collection and Structure Determination*

Single-crystal XRD data for **1**–**3** were collected on a Bruker Smart 1000 CCD diffractometer at 183(2) K with $Mo_{K\alpha}$ radiation ($\lambda = 0.71073$ Å). The program SAINT[8] was used for integration of the diffraction profiles. All the structures were solved by direct methods with the SHELXS program of the SHELXTL package and refined by full-matrix least-squares methods with SHELXL (semiempirical absorption corrections were applied with the SADABS program).[9] Metal atoms in each complex were located from the *E* maps, and other non-hydrogen atoms were located in successive difference Fourier syntheses and refined with anisotropic thermal parameters on $F^2$. The hydrogen atoms of the ligand were generated theoretically onto the specific atoms and refined isotropically with fixed thermal factors. The hydrogen atoms of the water molecules were located by the difference Fourier method. Further details of the structural analysis are summarized in Table 1.

CCDC-288377 (**1**), -267261 (**2**), and -267262 (**3**) contain the supplementary crystallographic data for this paper. These data can be obtained free of charge from the Cambridge Crystallographic Data Centre, 12 Union Road, Cambridge CB2 1EZ, UK (fax: (+44) 1223-336-033; e-mail: deposit@ccdc.com.ac.uk) or at www.ccdc.cam.ac.uk/data_request.cif.

## Acknowledgements

We thank Ms. Midori Goto for single-crystal XRD measurements and the AIST, Kobe University, and the JSPS for financial support. R.-Q. Zou is a JSPS research fellow (DC).

[1] a) M. Eddaoudi, J. Kim, N. Rosi, D. Vodak, J. Wachter, M. O'Keeffe, O. M. Yaghi, *Science* **2002**, *295*, 469; b) N. L. Rosi, J. Eckert, M. Eddaoudi, D. T. Vodak, J. Kim, M. O'Keeffe, O. M. Yaghi, *Science* **2003**, *300*, 1127; c) S. S. Kaye, J. R. Long, *J. Am. Chem. Soc.* **2005**, *127*, 6506; d) B. Chen, N. W. Ockwig, A. R. Millward, D. S. Contreras, O. M. Yaghi, *Angew. Chem.* **2005**, *117*, 4823; *Angew. Chem. Int. Ed.* **2005**, *44*, 4745; e) W. Mori, T. Sato, T. Ohmura, C. N. Kato, T. Takei, *J. Solid State Chem.* **2005**, *178*, 2555; f) R. Matsuda, R. Kitaura, S. Kitagawa, Y. Kubota, R. V. Belosludov, T. C. Kobayashi, H. Sakamoto, T. Chiba, M. Takata, Y. Kawazoe, Y. Mita, *Nature* **2005**, *436*, 238; g) S. R. Batten, R. Robson, *Angew. Chem.* **1998**, *110*, 1558; *Angew. Chem. Int. Ed.* **1998**, *37*, 1460; h) L. Pan, M. B. Sander, X. Y. Huang, J. Li, M. Smith, E. Bittner, B. Bockrath, J. K. Johnson, *J. Am. Chem. Soc.* **2004**, *126*, 1308; i) L. Pan, H. M. Liu, G. X. Lei, X. Y. Huang, D. H. Olson, N. J. Turro, J. Li, *Angew. Chem.* **2003**, *115*, 560; *Angew. Chem. Int. Ed.* **2003**, *42*, 542; j) J. Fan, W. Y. Sun, T. Okamura, W. X. Tang, N. Ueyama, *Inorg. Chem.* **2003**, *42*, 3868; k) T. K. Maji, K. Uemura, H. C. Chang, R.

  

Matsuda, S. Kitagawa, *Angew. Chem.* **2004**, *116*, 3331; *Angew. Chem. Int. Ed.* **2004**, *43*, 3269.

[2] E. Tynan, P. Jensen, P. E. Kruger, A. C. Lees, *Chem. Commun.* **2004**, 776.

[3] a) P. J. Steel, *Acc. Chem. Res.* **2005**, *38*, 243; b) X. C. Huang, J. P. Zhang, Y. Y. Lin, X. M. Chen, *Chem. Commun.* **2005**, 2232; c) C. J. Sumby, P. J. Steel, *New J. Chem.* **2005**, *29*, 1077.

[4] a) S. I. Nishikiori, H. Yoshikawa, Y. Sano, T. Iwamoto, *Acc. Chem. Res.* **2005**, *38*, 227; b) S. Masaoka, D. Tanaka, Y. Nakanishi, S. Kitagawa, *Angew. Chem.* **2004**, *116*, 2584; *Angew. Chem. Int. Ed.* **2004**, *43*, 2530.

[5] a) O. R. Evans, R. G. Xiong, Z. Wang, G. K. Wong, W. Lin, *Angew. Chem.* **1999**, *111*, 557; *Angew. Chem. Int. Ed.* **1999**, *38*, 536; b) I. S. Lee, D. M. Shin, Y. K. Chung, *Chem. Eur. J.* **2004**, *10*, 3158.

[6] a) B. Moulton, M. J. Zaworotko, *Chem. Rev.* **2001**, *101*, 1629; b) A. L. Pickering, G. Seeber, D. L. Long, L. Cronin, *Chem. Commun.* **2004**, 136; c) X. Yang, J. D. Ranford, J. Vittal, *Cryst. Growth Des.* **2004**, *4*, 781; d) A. Galet, M. C. Munoz, V. Martinez, J. A. Real, *Chem. Commun.* **2005**, 2268; e) E. Tynan, P. Jensen, N. R. Kelly, P. E. Kruger, A. C. Lees, B. Moubaraki, K. S. Murray, *Dalton Trans.* **2004**, 3440; f) S. Takamizawa, E. Nakata, H. Yokoyama, K. Mochizuki, W. Mori, *Angew. Chem.* **2003**, *115*, 4467; *Angew. Chem. Int. Ed.* **2003**, *42*, 4331; g) K. Takaoka, M. Kawano, M. Tominaga, M. Fujita, *Angew. Chem.* **2005**, *117*, 2189; *Angew. Chem. Int. Ed.* **2005**, *44*, 2151 and references therein.

[7] a) G. Férey, C. Mellot Draznieks, C. Serre, F. Millange, *Acc. Chem. Res.* **2005**, *38*, 217; b) L. Y. Kong, Z. H. Zhang, H. F. Zhu, H. Kawaguchi, T. Okamura, M. Doi, Q. Chu, W. Y. Sun, N. Ueyama, *Angew. Chem.* **2005**, *117*, 4426; *Angew. Chem. Int. Ed.* **2005**, *44*, 4352; c) O. R. Evans, W. Lin, *Acc. Chem. Res.* **2002**, *35*, 511; d) C. Y. Su, A. M. Goforth, M. D. Smith, H. C. zur Loye, *Chem. Commun.* **2004**, 2158; e) J. P. Zhang, Y. Y. Lin, X. C. Huang, X. M. Chen, *Chem. Commun.* **2005**, 1258 and references therein; f) Y.-L. Liu, V. Kravtsov, R. D. Walsh, P. Poddar, H. Srikanthc, M. Eddaoudi, *Chem. Commun.* **2004**, 2806; g) B. Kesanli, Y. Cui, M. R. Smith, E. W. Bittner, B. C. Bockrath, W. Lin, *Angew. Chem.* **2005**, *117*, 74; *Angew. Chem. Int. Ed.* **2005**, *44*, 72.

[8] Bruker AXS, SAINT Software Reference Manual, Madison, WI, **1998**.

[9] G. M. Sheldrick, SHELXTL NT Version 5.1, Program for Solution and Refinement of Crystal Structures, University of Göttingen, Göttingen (Germany), **1997**.

[10] D. M. Proserpio, R. Hoffmann, P. Preuss, *J. Am. Chem. Soc.* **1994**, *116*, 9634.

[11] P. S. Mukherjee, S. Konar, E. Zangrando, T. Mallah, J. Ribas, N. R. Chaudhuri, *Inorg. Chem.* **2003**, *42*, 2695.

[12] Y. H. Liu, H. C. Wu, H. M. Lin, W. H. Hou, K. L. Lu, *Chem. Commun.* **2003**, 60.

[13] V. A. Blatov, L. Carlucci, G. Cianib, D. M. Proserpio, *CrystEngComm* **2004**, *6*, 378.

[14] I. A. Baburina, V. A. Blatov, L. Carluccib, G. Cianib, D. M. Proserpio, *J. Solid State Chem.* **2005**, *178*, 2452.

[15] J. Zhang, W. Lin, Z. F. Chen, R. G. Xiong, B. F. Abrahams, H. K. Fun, *J. Chem. Soc. Dalton Trans.* **2001**, 1806.

[16] C. Klein, E. Graf, M. W. Hosseini, A. De Cian, *New J. Chem.* **2001**, *25*, 207.

[17] X. L. Wang, C. Qin, E. B. Wang, L. Xu, Z. M. Su, C. W. Hu, *Angew. Chem.* **2004**, *116*, 5146; *Angew. Chem. Int. Ed.* **2004**, *43*, 5036.

[18] a) *Photochemistry and Photophysics of Coordination Compounds* (Eds.: H. Yersin, A. Vogler), Springer, Berlin, **1987**; b) B. Valeur, *Molecular Fluorescence: Principles and Application*, Wiley-VCH, Weinheim, **2002**.

[19] Implemented as the PLATON procedure: A. L. Spek, *A Multipurpose Crystallographic Tool*, Utrecht University, Utrecht (The Netherlands), **1998**.

[20] M. J. Frisch, G. W. Trucks, H. B. Schlegel, G. E. Scuseria, M. A. Robb, J. R. Cheeseman, J. A. Montgomery, Jr., T. Vreven, K. N. Kudin, J. C. Burant, J. M. Millam, S. S. Iyengar, J. Tomasi, V. Barone, B. Mennucci, M. Cossi, G. Scalmani, N. Rega, G. A. Petersson, H. Nakatsuji, M. Hada, M. Ehara, K. Toyota, R. Fukuda, J. Hasegawa, M. Ishida, T. Nakajima, Y. Honda, O. Kitao, H. Nakai, M. Klene, X. Li, J. E. Knox, H. P. Hratchian, J. B. Cross, C. Adamo, J. Jaramillo, R. Gomperts, R. E. Stratmann, O. Yazyev, A. J. Austin, R. Cammi, C. Pomelli, J. W. Ochterski, P. Y. Ayala, K. Morokuma, G. A. Voth, P. Salvador, J. J. Dannenberg, V. G. Zakrzewski, S. Dapprich, A. D. Daniels, M. C. Strain, O. Farkas, D. K. Malick, A. D. Rabuck, K. Raghavachari, J. B. Foresman, J. V. Ortiz, Q. Cui, A. G. Baboul, S. Clifford, J. Cioslowski, B. B. Stefanov, G. Liu, A. Liashenko, P. Piskorz, I. Komaromi, R. L. Martin, D. J. Fox, T. Keith, M. A. Al-Laham, C. Y. Peng, A. Nanayakkara, M. Challacombe, P. M. W. Gill, B. Johnson, W. Chen, M. W. Wong, C. Gonzalez, J. A. Pople, Gaussian 03 (Revision B.04), Gaussian, Inc., Pittsburgh (USA), **2003**.

[21] a) C. Lee, W. Yang, R. G. Parr, *Phys. Rev. B* **1988**, *37*, 785; b) A. D. Becke, *J. Chem. Phys.* **1993**, *98*, 5648.

[22] a) A. D. McLean, G. S. Chandler, *J. Chem. Phys.* **1980**, *72*, 5639; b) R. Krishnan, J. S. Binkley, R. Seeger, J. A. Pople, *J. Chem. Phys.* **1980**, *72*, 650; c) M. J. Frisch, J. A. Pople, J. S. Binkley, *J. Chem. Phys.* **1984**, *80*, 3265; d) P. J. Hay, W. R. Wadt, *J. Chem. Phys.* **1985**, *82*, 299.

Received: April 14, 2006
Published online: September 8, 2006

  